A Novel Iodomethylene-dimethyl-dihydropyranone Induces G_2/M Arrest and Apoptosis in Human Cancer Cells

JÉRÔME BIGNON, MICHEL BÉNÉCHIE, DENYSE HERLEM, JIAN-MIAO LIU, ALEXIA PINAULT, FRANÇOISE KHUONG-HUU and JOANNA WDZIECZAK-BAKALA

Institut de Chimie des Substances Naturelles, Centre National de la Recherche Scientifique, 91190 Gif-sur-Yvette, France

Abstract. *Background: The putative pharmacophore of a naturally cytotoxic limonoid haperforin B1, E-5-iodomethylene-6,6-dimethyl-5,6-dihydropyran-2-one (IDDP) was synthesized and its biological activity was investigated. Materials and Methods: The cytotoxicity of IDDP was assessed using human breast, lung, colorectal and epidermal carcinomas, chronic myeloid leukemia and glioblastoma cell lines. Cell cycle analysis was performed by flow cytometry. The induction of apoptosis was studied by a caspase assay and by annexin V-propidium iodide double staining. The organization of actin and tubulin microfilaments was analysed by immunocytochemical labeling. Results: IDDP was shown to inhibit the growth of a panel of human cancer cell lines independently of their p53 status with IC_{50} ranging from 0.07 to 0.50 μM. All the treated cells were arrested in the G_2/M phase in a time-dependent manner before cell death occurred through an apoptotic pathway. Immunocytochemical studies revealed that the normal organization of microfilaments and microtubules was disrupted in IDDP exposed cells. Conclusion: IDDP can be considered as a promising anticancer agent.*

Over the past decades, chemotherapy, either alone or in association with surgery and/or radiotherapy, has maintained major importance for the treatment of cancer. However, progressive neoplasic diseases still remain one of the leading causes of death in developed countries. The efficiency of many clinically used anticancer drugs is limited by their toxicities and by intrinsic or acquired drug resistance (1, 2). Thus, there is a critical need for new therapies with improved potency over current treatments, especially against refractory tumors. It has been reported that the antitumor efficacy of several chemotherapeutic molecules correlates with their apoptosis-inducing ability (3). Therefore, it appears essential to identify new compounds able to induce the apoptotic death of tumor cells and overcome the frequently developed tumor resistance to conventional anticancer drugs.

The search for antitumor compounds is ongoing over the world. A great number of investigations have focused on the identification of phytochemicals able to inhibit the growth of cancer cells, and several *in vitro* and *in vivo* studies have shown that extracts from a number of medicinal plants have anticancer potential (4-8). *Harrisonia perforata* (*Blanco*) Merr. belonging to the family of *Simaroubaceae* is a common bush widely distributed in Southeast Asia. Chemical composition analysis of the leaves of this plant has revealed the presence of several limonoids belonging to the obacunol series (9). We have previously isolated nine new limonoids (10-12) from the leaves of *Harrisonia perforata* (*Simaroubaceae*) originated from Central Vietnam. The structure of haperforin B1 (Figure 1), one of the isolated limonoids, presents a complex ring-cleaved rearranged skeleton of the parent tetranortriterpenoid (9). Preliminary biological studies of haperforin B1 suggested its cytotoxic activity. During the course of chemical synthesis of haperforin B1, the intermediate product, E-5-iodomethylene-6,6-dimethyl-5,6-dihydropyran-2-one (IDDP), which is more toxic to cancer cell lines than haperforin B1 was discovered. This unsaturated δ-lactone moiety of haperforin B1 bearing an acrylic side chain represents an unusual structural element and a possible pharmacophore.

A short synthesis of IDDP is described and its *in vitro* anti-proliferative activity against several chemosensitive and resistant cancer cell lines as well as its ability to induce cell death by apoptosis was investigated.

Materials and Methods

Chemistry. Unless otherwise indicated, all commercially available foundational materials were used directly without further purification. Reactions requiring anhydrous conditions were performed in dried and distilled solvents under argon atmosphere. All the reactions were

This paper is dedicated to the memory of Pierre Potier.

Correspondence to: Jérôme Bignon, ICSN, CNRS, 91198 Gif-sur-Yvette, France. Tel: +33 169823048, Fax: +33 169077247, e-mail: Jerome.Bignon@icsn.cnrs-gif.fr

Key Words: Cancer, haperforin, chemotherapy, apoptosis, cell cycle, cytoskeleton.

monitored by thin layer chromatography (TLC) performed on silica gel 60 F_{254} plates from Merck Chemicals (Darmstadt, GER). Column chromatography was performed using Merck Kieselgel 60H. ^{1}H and ^{13}C nuclear magnetic resonance (NMR) spectra were measured on a Bruker spectrometer Avance 300 instrument (Bruker BioSpin, Ettlinger, GER) using the indicated solvent. Chemical shifts (δ) are expressed in part per million (ppm) with tetramethylsilane (TMS) as internal standard. Signal multiplicities are indicated by the following abreviations: s (singlet), d (doublet) and br (broad peak) were used, coupling constants (J), were expressed in hertz (Hz). Infrared (IR) spectra were recorded with a Perkin Elmer Spectrum BX FT IR spectrometer (Waltham, MA, USA) in liquid film on sodium chloride plates. Wave numbers (ν) are given in cm^{-1}. Electrospray ionization (ESI) mass spectra in the high resolution mode (HRMS) were recorded with an LCT (Micromass) spectrometer (Waters corp., MA, USA). m/z is the abreviation used for mass-to-charge ratio. Ultraviolet (UV) spectra were recorded with a Varian Cary 100 spectrometer (Palo Alto, CA, USA). Wavelength (λ) in a given solvent is expressed in nanometer (nm), ε being the molar absorption coefficient.

(2E)-2-Iodomethylene-3-methylbutane-1,3 diol ***2***. To a solution of the ester ethyl (2Z)-3-hydroxy-2-(iodomethylene)-3-methyl butanoate **1** (13, 14) (1.4 g, 4.9 mmol) in dry tetrahydrofuran (THF), (30 mL) was added lithium aluminium hydride (LiAlH4), (112 mg, 2.9 mmol). The resulting mixture was stirred at room temperature for 1 h. After hydrolysis with a saturated solution of sodium sulfate, the resulting mixture was filtered through a pad of celite which was washed with chloroform (2×20 mL). The combined phases were dried over magnesium sulfate and concentrated under vacuum to afford the diol **2** as a white solid (900 mg, 75%). ^{1}H NMR (300 MHz, $CDCl_3$): δ (ppm) 1.42 (s, 6H); 4.44 (s, 2H); 6.48 (s, 1H).

(2Z)-3-hydroxy-2-(iodomethylene)-3-methyl butanal ***3***. To a solution of the allylic alcohol **2** (1.4 g, 4.7 mmol) in dry dichloromethane (CH_2Cl_2) (30 mL) was added activated manganese dioxide (MnO_2), (5g, 10 equivalents) in small portions. The resulting mixture was stirred at room temperature until no original material could be detected by TLC. The resulting mixture was filtered through a pad of celite which was washed with CH_2Cl_2 (2×20 mL). The combined phases were concentrated under vacuum to afford the aldehyde **3** as a pale yellow oil (1.34 g, 96%). ^{1}H NMR (300 MHz, $CDCl_3$): δ (ppm) 1.43 (s, 6H); 7.97 (s, 1H); 9.79 (s, 1H). ^{13}C NMR (75.5 MHz, $CDCl_3$): δ (ppm) 28.67, (2 C); 74.16; 101.81; 149.96; 196.84. IR (film) ν max (cm^{-1}) 1681; 1565; 1456; 1369; 1282.

*(5E)-5-iodomethylene-6,6-dimethyl-5,6-dihydropyran-2-one (****IDDP****)*. A mixture of potassium carbonate (K_2CO_3), (4.48 g, 32 mmol) and 18-crown-6 / acetonitrile complex (15) (17.1 g, 64.8 mmol) in freshly distilled toluene (54 mL) was kept under argon and stirred for 1 h at room temperature (RT) then cooled to –20˚C. To this solution were added the aldehyde **3** (1.3 g, 5.4 mmol) followed by methyl (*bis*(2,2,2-trifluoroethyl)-phosphinoyl)-acetate (1.72 g, 5.4 mmol) (16). This mixture was stirred for 30 min at –20˚C, then 1 h at 0˚C. The reaction was quenched by the addition of an aqueous solution of ammonium chloride (NH4Cl). After extraction with ether (3×50 mL), the combined organic phases were dried over magnesium sulfate ($MgSO_4$) and concentrated under vacuum to give a yellow green solid. Silica gel column chromatography (heptane/ether=95/5) afforded IDDP (1.06g, 74%) as a white solid. ^{1}H NMR (300 MHz, $CDCl_3$): δ (ppm) 1.62 (s, 6H); 6.1 (dd, J=10Hz, J=2Hz, 1H); 6.88 (br s, ^{1}H); 7.2 (dd, J=10 Hz, J=1 Hz , 1H). ^{13}C NMR (75.5 MHz, $CDCl_3$): δ (ppm) 28.9, (2 C); 84.0; 86.4; 121.61; 142.26; 145; 163.28. IR (film) ν_{max} (cm^{-1}) 1695; 1560; 1394; 1290; 1115. UV (EtOH) λ (nm): 300. Log ε=4.1. HRMS (ESI): m/z=286.9530 $(M+Na)^+$; calculation for $C_8H_9O_2NaI$ 286.9545.

The synthesis of IDDP is summarized in Figure 2 and the yield from **2** was 50% .

Cell culture and proliferation assay. Cancer cell lines were obtained from the American Type Culture Collection (Rockville, MD, USA) and were cultured according to the supplier's instructions. Briefly, human KB epidermal carcinoma cells were grown in Eagle's minimal essential medium (EMEM) containing 4.5 g/L glucose supplemented with 10% fetal calf serum (FCS) and 1% glutamine. Human A549 and H1299 lung carcinomas, U87 glioma and MDA-MB231 and MCF7 breast carcinoma cells were grown in Dulbecco's minimal essential medium (DMEM) containing 4.5 g/L glucose supplemented with 10% FCS and 1% glutamine. Human K562 chronic myelogenous leukemia and HCT116 colorectal carcinoma cells were grown in RPMI 1640 containing 10% FCS and 1% glutamine. The doxorubicin-resistant variant of the K562 leukemic cell line (K562-ADR) was a generous gift from Pr J.P. Marie (Paris, France). All the cell lines were maintained at 37˚C in a humidified atmosphere containing 5% CO_2. Cell viability was assessed using Promega CellTiter-Blue™ reagent (Promega, Madison, WI, USA) according to the manufacturer's instructions. Briefly, the cells were seeded in 96-well plates (5×10^3 cells/well) containing 50 μl of growth medium. After 24 h of culture, the cells were supplemented with 50 μl of IDDP or haperforin B1 dissolved in DMSO (less than 0.1% in each preparation). After 72 h of incubation, 20 μl of resazurin was added for 2 h before recording fluorescence (560 nm Ex/590 nm Em) using a Victor microtiter plate fluorimeter (Perkin-Elmer). The IC_{50} corresponds to the concentration of IDDP that induced a 50% decrease in fluorescence of drug-treated cells compared with untreated cells. All experiments were performed in triplicate.

Cell cycle analysis. Exponentially growing cancer cells (K562, HCT116, H1299 and MDA-MB231) were incubated with tested compound or DMSO for 24 h. Cell-cycle profiles were determined by flow cytometry on a FC500 flow cytometer (Beckman-Coulter, Villepinte, France) as described previously (17).

Apoptosis assay. Apoptosis was measured by the Apo-one homogeneous caspase-3/7 assay (Promega) according to the manusfacturer's recommendations. The cleavage of pro-caspases to active caspases is one of the hallmarks of apoptosis. Briefly the K562, HCT116, H1299 and MDA-MB231 cells were sub-cultured on a 96-well plate with 5×10^4 cells/well in 100 μl medium. After 24 h of incubation, the medium in the 96-well plate was discarded and replaced with medium containing different concentrations of IDDP (0.05, 0.1 or 0.5 μM) or 0.1% DMSO (as negative control). After 24 h of treatment, 100 μl of a mixture of caspase substrate and Apo-one caspase 3/7 buffer were added to each well. One hour later, the activity of caspase 3 and 7 was evaluated by measuring the fluorescence of the samples at λ=527 nm using a Victor microtiter plate fluorimeter (Perkin-Elmer).

The apoptosis of IDDP-treated K562 cells was also assessed by flow cytometry using propidium iodide (PI) and an Annexin-V-

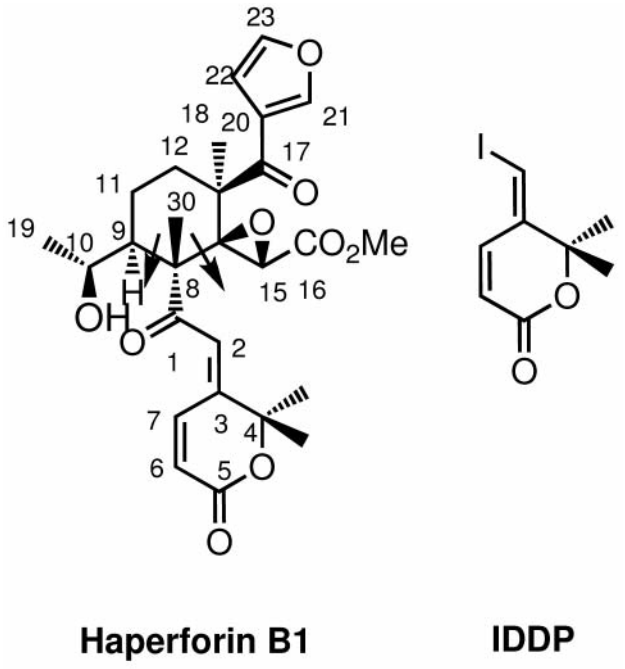

Figure 1. *Structure of haperforin B1 (9) and IDDP.*

FITC apoptosis detection kit (BD Biosciences, San Jose, CA, USA) according to the manufacturer's instructions. FITC-conjugated annexin V has been used to detect the externalization of phosphatidylserine that occurs at an early stage of apoptosis. PI is currently used as a marker for necrosis due to cell membrane destruction.

Immunocytochemistry. MDA-MB231 cells cultured on a Lab-Tek chamber slide (VWR International, Strasbourg, France) were treated with 0.5 μM of IDDP for 24 h. At the end of the treatment, the cells were washed once with PBS prior to fixation with 3.7% formaldehyde for 20 min. The fixed cells were washed 3 times in PBS, and then permeabilized with 0.1% Triton® X-100 in PBS for 3 min at room temperature. The cells were washed 3 times in PBS and preincubated for 1 h in a solution of PBS containing 1% BSA (bovin serum albumin) and 10% goat serum to block nonspecific antibody binding, prior to incubation for 12 h at 4˚C with the mouse anti-β tubulin antibody (1:100) (Invitrogen, Eragny-sur-Oise, France). Cells incubated with PBS/1% BSA instead of primary antibody were used as negative control. At the end of incubation, the cells were washed 3 times in PBS containing 1% BSA and incubated for 2 h at room temperature with FITC-labeled goat anti-mouse antibody (1:100) (Invitrogen), Tetra-methyl-rhodamine-iso-thio-cyanate (TRITC)-labeled-phalloidin which binds selectively to F-actin was used for actin staining (1:40) (Invitrogen) and Hoechst 33342 for nuclear staining (1:5000) (Invitrogen). At the end of incubation, the cells were washed once in PBS and mounted in fluorescent mounting medium (Dako, Trappes, France). Images were acquired using a Nikon TE2000E fluorescent microscope (Nikon, Champigny-sur-Marne, France) equipped with a Nikon DXM1200F digital camera.

Table I. *Cytotoxicity (IC_{50}) of IDDP and haperforin B1.*

Cell line	IDDP	haperforin B1
KB	0.45±0.01	15±0.12
HCT116	0.28±0.03	16±0.18
U87	0.18±0.05	3±0.24
A549	0.44±0.12	20±0.36
MCF7	0.33±0.07	22±0.20
H1299	0.39±0.03	Nd
MDA-MB231	0.50±0.13	Nd
K562	0.15±0.02	Nd
K562-ADR	0.07±0.03	Nd

IC_{50} represents the concentration (μM) of the studied compound required to inhibit 50% of cell growth after 72 h of treatment. Data are the mean±standard error (SEM) of three independent experiments. Nd, Not determined.

Table II. *Percentage of K562, HCT116, H1299 and MDA-MB231 cancer cells in the G_2/M phase after 24 h of treatment with IDDP.*

Concentration of IDDP (μM)	K562 (% G_2/M)	HCT116 (% G_2/M)	H1299 (% G_2/M)	MDA-MB 231 (% G_2/M)
Control	14.5	28.4	15.9	26.2
0.05	13.9	25.5	17.5	29.4
0.1	18.0	29.2	24.8	31.7
0.2	52.3	54.2	32.7	32.4
0.5	76.9	Nd	66.7	59.4

Data shown are representative of three independent experiments with similar results. Nd: Not determined.

Tubulin assembly and disassembly. Inhibition of tubulin polymerization and depolymerization was measured as previously described (18, 19).

Results

Effect of IDDP on cell proliferation. As shown in Table I, the IC_{50} of IDDP ranged from 0.07 to 0.50 μM, clearly indicating an antiproliferative activity regardless of the origin of the tumor cells (colon, lung, cervical carcinomas, glioblastoma, leukemia, oestrogen-dependent and independent breast carcinomas), with a maximal efficacy against U87 glioblastoma (IC_{50}=0.18 μM) and K562 leukemia (IC_{50}=0.15 μM) cells. IDDP was also shown to inhibit the proliferation of the doxorubicin-resistant K562-ADR leukemic cell line with an IC_{50} of 0.07 μM.

Effect of IDDP on the cell cycle. After 24 h treatment with 0.2 μM of IDDP, a significant increase in the number of cells arrested at the G_2/M growth phase was observed (Table II). Increasing the concentration of IDDP to 0.5 μM led to

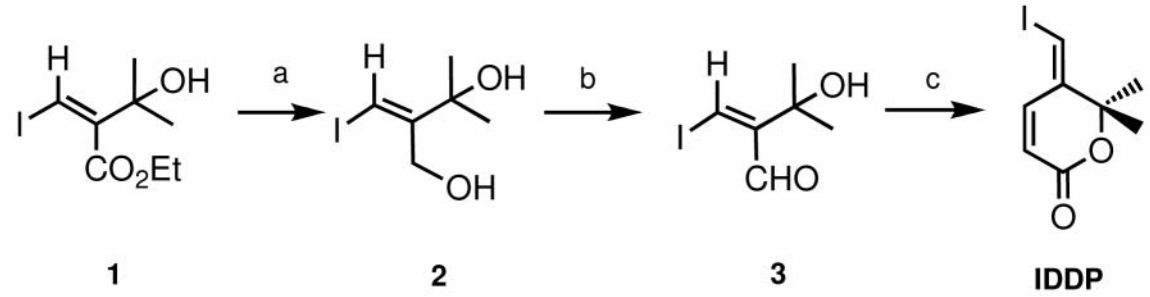

Figure 2. *Reaction conditions: a-$LiAlH_4$, 1 eq, ether, RT, 1 h, 75% ; b-MnO_2, 10 eq, CH_2Cl_2, 3 h, 96% ; c-K_2CO_3, 6 eq, 18-crown-6/CH_3CN, 12 eq, toluene, 25˚C, 1 h, then –20˚C,* ***3*** *1 eq and $(CF_3CH_2O)2$-P(O)-CH_2CO_2Me, 1 eq., 30 min, then 0˚C, 1 h, 74% .*

essentially the same result in all the treated cells. In all the cells exposed to IDDP for 24 h, a sub-diploid DNA content was observed (data not shown) indicating that the cells were undergoing apoptosis.

Apoptotic death. The ability of IDDP to induce apoptosis was further investigated using a specific apoptosis assay. IDDP induced apoptosis as shown by caspase cleavage in all the investigated cell lines (Figure 3). In particular, an 8-fold increase in apoptosis in the H1299 non-small lung human carcinoma and a 4.5-fold increase in apoptosis in the K562 leukemia cells was observed. Treatment of the K562 cells with either 0.1 μM or 0.5 μM IDDP induced the appearance of PI-negative/annexin V-positive cells (22.1% and 49.1% , respectively, as compared to 6.8% for control cells treated with 0.1% DMSO).

Morphological changes and actin/tubulin reorganization. Light microscopy examination of K562 cells exposed to IDDP provided additional proof of the cytotoxic effect of this compound. As shown in Figure 4, K562 cells treated with IDDP underwent morphological changes from a round appearance to an elongated shape. As early as 4 h after treatment with 0.5 μM IDDP, the morphology of the MDA-MB231 cells was modified and it was clearly shown that IDDP caused cellular microtubule abnormal organization and arrangement in studied cells (Figure 5). As shown in Figure 5A, the changes in F-actin distribution were present shortly after treatment (4 h). This effect was amplified following 24 h treatment (Figure 5B) and the inhibition of cellular proliferation was accompanied by the appearance of numerous fragmented nuclei in the apoptotic cells (Figure 6).

Effect of IDDP on tubulin polymerization/depolymerisation. IDDP did not prevent tubulin assembly (12% of inhibition observed in the presence of 1 mM IDDP as compared to 50% obtained with 2.5 μM colchicine) or disassembly (2% of inhibition observed in the presence of 1 mM IDDP as compared to 50% obtained with 0.5 μM Taxol®).

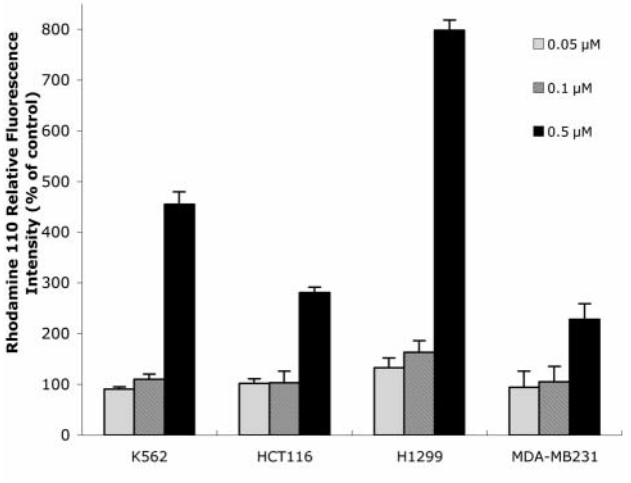

Figure 3. *Dose-dependent apoptosis induced by IDDP in different cancer cell lines following 24-hours treatment.*

Discussion

The IC_{50} values obtained with all the cell lines indicated that IDDP had higher proliferative activity than haperforin B1. *In vitro* IDDP treatment led to a significant dose-dependent cell cycle arrest in the G2/M phase and to an induction of apoptosis in a time- and dose-dependent manner in a wide range of cancer cells with different p53 status, for example in wild-type p53 (HCT116) as well as in p53-deficient cancer cells (H1299). The results also provide evidence that IDDP induced the death of K562 leukemic cells which are resistant to the induction of apoptosis by a variety of different agents, including diphtheria toxin, camptothecin, cytarabine, etoposide, paclitaxel, staurosporine and anti-Fas antibodies (20-25).

It is well known that both actin and microtubule cytoskeletal systems play key roles in cellular processes including the generation and maintenance of cell morphology and polarity, in endocytosis and intracellular trafficking, and in contractility, motility and cell division (26, 27). The

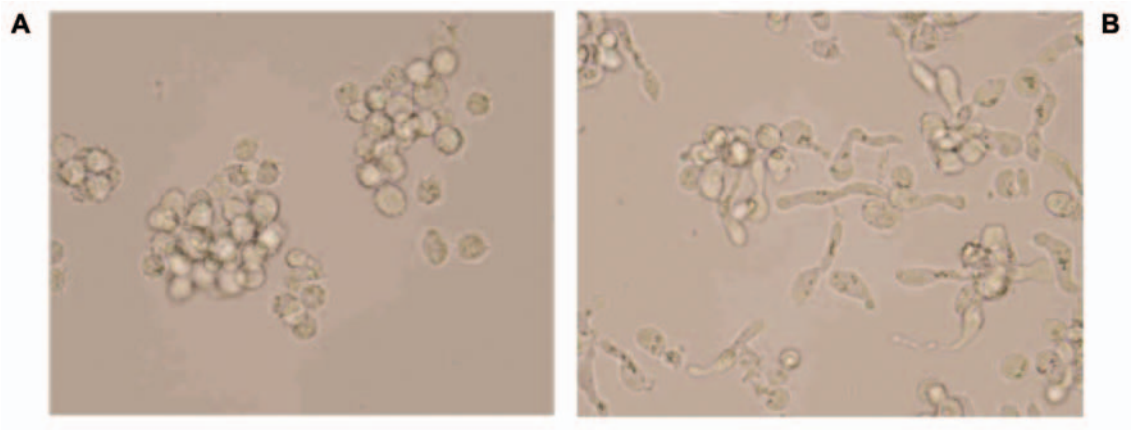

Figure 4. *Effect of IDDP on the morphology of K562 cells following 24 h treatment with (A) 0.1% DMSO and (B) 0.5 μM IDDP (×40).*

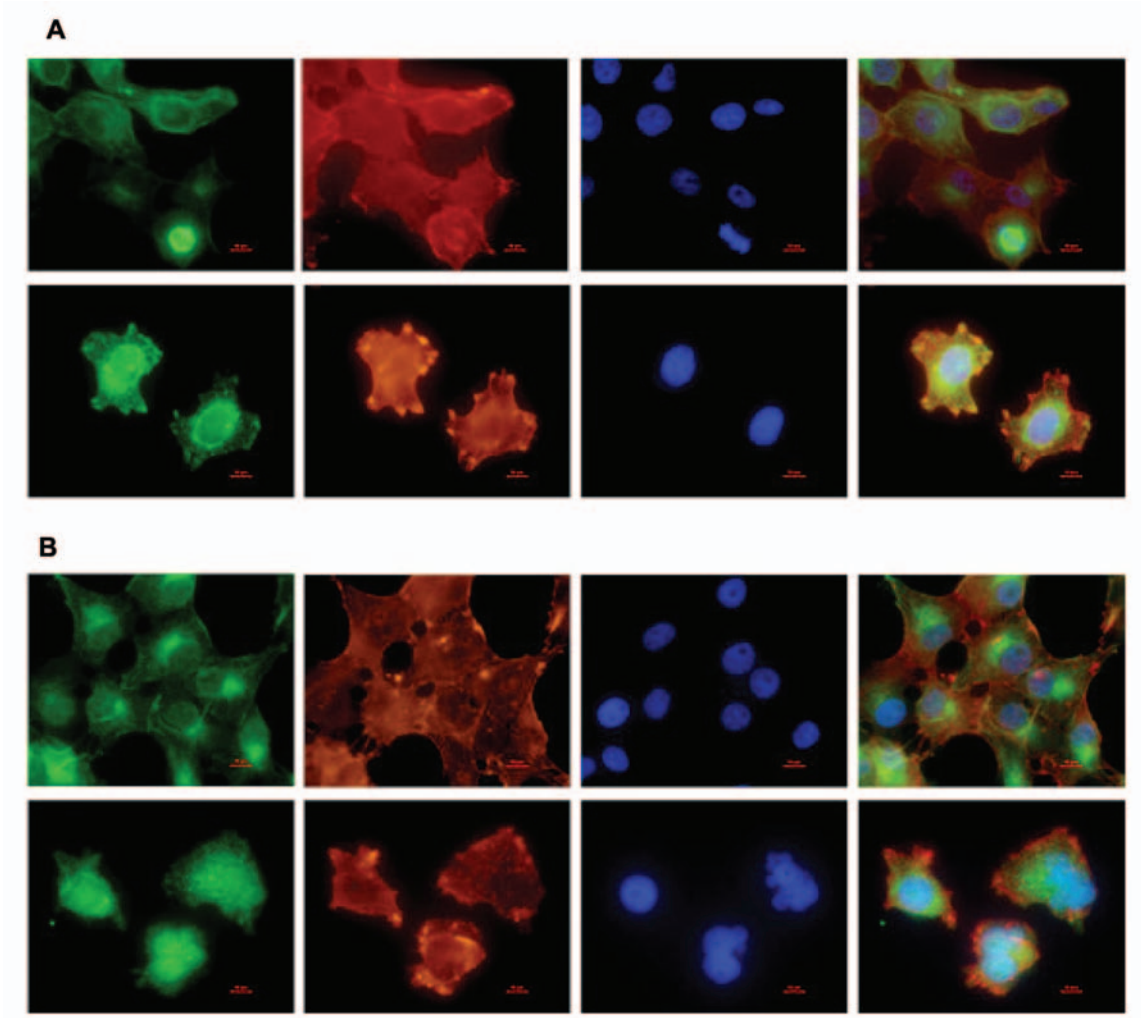

Figure 5. *Cytoskeletal disruptions and morphological changes in MDA-MB231 cells treated (bottom panel) for 4 (A) or 24 h (B) with 0.5 μM IDDP; control cells (upper panel). Nuclei stained with Hoechst 33342 (blue), actin filaments stained with TRITC-labeled-phalloidin (red), microtubules labeled with a primary mouse anti-β-tubulin monoclonal antibody and FITC-conjugated goat anti mouse IgG (green) (×100). Scale bar, 10 μm.*

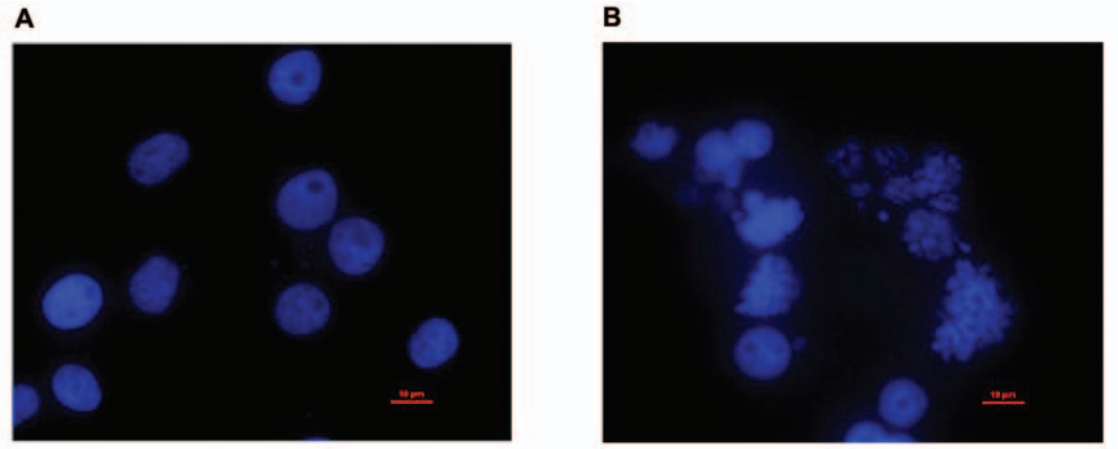

Figure 6. *Fluorescence images of control (A) and apoptotic MDA-MB 231 cells (B) obtained following 24 h treatment with 0.5 μM IDDP. Nuclei stained with Hoechst 33342; typical features of IDDP treated cells were condensed chromosomes, numerous fragmented micronuclei and apoptotic bodies (×100). Scale bar, 10 μm.*

changes in cell shape suggested that IDDP interrupt cell division during mitosis or cytokinesis. In fact, it was previously reported that changes in cell shape were associated with reorganization of actin filaments (28, 29). Moreover, because microfilaments as well as microtubules are essential for cell division, and their disruption can induce G_2/M arrest and apoptosis (30, 31), triple fluorescence labeling was employed to analyse cell morphology. IDDP disrupted the microtubule dynamics with tubulin depolymerization and perturbed the normal organization of the microfilaments, accompanied by the alteration of cell shape, by aberrant mitosis and apoptosis in the targeted cells.

In order to understand how IDDP induced these cellular changes and to identify its molecular target(s), the capacity of IDDP to act as a tubulin binder was evaluated *in vitro*. Many clinically used conventional anticancer drugs inhibit mitosis through direct interference with tubulin dynamics. However IDDP did not directly inhibit either the tubulin polymerisation or depolymerisation. Taking into account the findings concerning the effect of IDDP on cell morphology, the possibility that IDDP directly interfered with the actin microfilaments and consequently altered microtubule organization could not be excluded. On the other hand, IDDP could have interacted with one of the proteins involved in the connection between actin and the tubulin cytoskeletons (32, 33). A role of Aurora A, B and C kinases in the signaling pathway of IDDP was excluded since no effect of IDDP on the activity of these kinases was observed (data not shown).

IDDP is characterized by toxicity towards cells overexpressing MDR1, the major protein implicated in chemoresistance (34, 35). The value of the calculated resistance factor (RF=0.47) also indicated that IDDP possesses greater antiproliferative potency against the K562 resistant cells than against the parent cells. These findings suggest that IDDP may overcome the MDR1-mediated chemoresistance in this cell line and does not represent a substrate for the P-glycoprotein. This property of IDDP remains of great clinical interest and indicates an expectation of significant antitumoral efficacy.

Because of the significant antiproliferative effect of IDDP observed *in vitro*, a pilot *in vivo* study of antitumor activity was developed using a murine xenograft model. The encouraging results indicated that IDDP reduced the size of the grafted tumors, albeit that these preliminary data were not statistically significant (data not shown). It is well known that the effect of the anticancer drug depends on its dose, route of administration and on its application intervals. To improve the antitumor efficacy of IDDP, various protocols of compound administration as well as different tumor models should be investigated. Additionally, the search for potential molecular target(s) of IDDP is under investigation.

Acknowledgements

The authors thank Dr R. Dodd for critical reading of the manuscript and Ms S. Thoret for her technical assistance. Jian-Miao Liu and Alexia Pinault were supported by a grant funded by the Institut de Chimie des Substances Naturelles, CNRS.

References

1 Gonzalez-Angulo AM, Morales-Vasquez F and Hortobagyi GN: Overview of resistance to systemic therapy in patients with breast cancer. Adv Exp Med Biol *608*: 1-22, 2007.

2 Baird RD and Kaye SB: Drug resistance reversal-are we getting closer? Eur J Cancer *39*: 2450-2461, 2003.

3 Yu CH, Kan SF, Pu HF, Jea Chien E and Wang PS: Apoptotic signalling in bufalin- and cinobufagin-treated androgen-dependent and -independent human prostate cancer cells. Cancer Sci *99*: 2467-2476, 2008.

4 Hu H, Ahn NS, Yang X, Lee YS and Kang KS: *Ganoderma lucidum* extract induces cell cycle arrest and apoptosis in MCF-7 human breast cancer cell. Int J Cancer *102*: 250-253, 2002.
5 Lee SM, Li ML, Tse YC, Leung SC, Lee MM, Tsui SK, Fung KKP, Lee CY and Wave MM: Paeoniae Radix, a Chinese herbal extract, inhibit hepatoma cells growth by inducing apoptosis in a p53 independent pathway. Life Sci *71*: 2267-2277, 2002.
6 Skupien K, Oszmianski J, Kostrzewa-Nowak D and Tarasiuk J: *In vitro* antileukaemic activity of extracts from berry plant leaves against sensitive and multidrug resistant HL60 cells. Cancer Lett *236*: 282-291, 2006.
7 Yang L, Wu S, Zhang Q, Liu F and Wu P: 23,24-Dihydrocucurbitacin B induces G_2/M cell-cycle arrest and mitochondria-dependent apoptosis in human breast cancer cells (Bcap37): Cancer Lett *256*: 267-278, 2007.
8 Aziz MH, Dreckschmidt NE and Verma AK: Plumbagin, a medicinal plant-derived naphthoquinone, is a novel inhibitor of the growth and invasion of hormone-refractory prostate cancer. Cancer Res *68*: 9024-9032, 2008.
9 Taylor DAH: The chemistry of the limonoids from *Meliaceae*. Prog Chem Org Nat Prod *45*: 1-102, 1984.
10 Chiaroni A, Riche C, Khuong-Huu Q, Nguyen-Ngoc H, Nguyen-Viet K and Khuong-Huu F: New limonoids from *Harrisonia perforata* (*Blanco*) Merr. Acta Cryst *C56*: 711-713, 2000.
11 Khuong-Huu Q, Chiaroni A, Riche C, Nguyen-Ngoc H, Nguyen-Viet K and Khuong-Huu F: New rearranged limonoids from *Harrisonia perforata*. J Nat Prod *63*: 1015-1018, 2000.
12 Khuong-Huu Q, Chiaroni A, Riche C, Nguyen-Ngoc H, Nguyen-Viet K and Khuong-Huu F: New rearranged limonoids from *Harrisonia perforata* III. J Nat Prod *64*: 634-637, 2001.
13 Ben Ayed T, Villieras J and Amri H: A stereoselective synthesis of α–(1-hydroxyalkyl)-β–substituted acrylic acid esters. Tetrahedron *56*: 805-809, 2000.
14 Wei HX, Gao J, Li G and Pare PW: Synthesis of β-iodo-α–(hydroxyalkyl) acrylates. Tetrahedron Lett *43*: 5677-5680, 2002.
15 Gokel GW, Cram DJ, Liotta CL, Harris HP and Cook FL: Preparation and purification of 18-crown-6. J Org Chem *39*: 2445-2446, 1974.
16 Still WC and Gennari C: Direct synthesis of Z-unsaturated esters. A useful modification of the Horner-Emmons olefination. Tetrahedron Lett *24*: 4405-4406, 1983.
17 Venot C, Maratrat M, Dureuil C, Conseiller E, Bracco L and Debussche L: The requirement for the p53 proline-rich functional domain for mediation of apoptosis is correlated with specific *PIG3* gene transactivation and with transcriptional repression. EMBO J *17*: 4668-4679, 1998.
18 Zavala F, Guenard D, Robin JP and Brown E: Structure-antitubulin activity relationships in *Steganacin congeners* and analogues. Inhibition of tubulin polymerization *in vitro* by (+/-) isodeoxypodophyllotoxin. J Med Chem *23*: 546-549, 1980.
19 Lataste H, Senilh V, Wright M, Guenard D and Potier P: Relationships between the structures of taxol and baccatine III derivatives and their *in vitro* action on the disassembly of mammalian brain and *Physarum* amoebal microtubules. Proc Natl Acad Sci USA *81*: 4090-4094, 1984.
20 Chang MP, Bramhall J, Graves S, Bonavida B and Wisnieski BJ: Internucleosomal DNA cleavage precedes diphtheria toxin-induced cytolysis. Evidence that cell lysis is not a simple consequence of translation inhibition. J Biol Chem *264*: 15261-15267, 1989.
21 McGahon A, Bissonnette R, Schmitt M, Cotter KM, Green DR and Cotter TG: Bcr-Abl maintains resistance of chronic myelogenous leukemia cells to apoptotic cell death. Blood *83*: 1179-1187, 1994.
22 McGahon AJ, Nishioka WK, Martin SJ, Mahboubi A, Cotter TG and Green DR: Regulation of the Fas apoptotic cell death pathway by Abl. J Biol Chem *270*: 22625-22631, 1995.
23 Gangemi RM, Tiso M, Marchetti C, Severi AB and Fabbi M: Taxol cytotoxicity of human leukemia cell lines is a function of their susceptibility to programmed cell death. Cancer Chemother Pharmacol *36*: 385-392, 1995.
24 Dubrez L, Goldwasser F, Genne P, Pommier Y and Solary E: The role of cell cycle regulation and apoptosis triggering in determining the sensitivity of leukemic cells to topoisomerase I and II inhibitors. Leukemia *9*: 1013-1024, 1995.
25 Ray S, Bullock G, Nunez G, Tang C, Ibrado AM, Huang Y and Bhalla K: Enforced expression of Bcl-xs induces differentiation and sensitizes chronic myelogenous leukemia-blast crisis K562 cells to 1-β-D-arabinofuranosylcytosine-mediated differentiation and apoptosis. Cell Growth Diff *7*: 1617-1623, 1996.
26 Barr FA and Gruneberg U: Cytokinesis: placing and making the final cut. Cell *131*: 847: 860, 2007.
27 Jaworski J, Hoogenraad CC and Akhmanova A: Microtubule plus-end tracking proteins in differentiated mammalian cells. Int J Biochem Cell Biol *40*: 619-637, 2008.
28 Burridge K and Chrzanowska-Wodnicka M: Focal adhesions, contractility, and signaling. Annu Rev Cell Dev Biol *12*: 463-518, 1996.
29 Gu YY, Zhang HY, Zhang HJ, Li SY, Ni JH and Jia HT: 8-Chloro-adenosine inhibits growth at least partly by interfering with actin polymerisation in cultured human lung cancer cells. Biochem Pharmacol *72*: 541-550, 2006.
30 Yamasaki Y, Tsuruga M, Zhou D, Fujita Y, Shang X, Dang Y *et al*: Cytoskeletal disruption accelerates caspase-3 activation and alters the intracellular membrane reorganization in DNA damage-induced apoptosis. Exp Cell Res *259*: 64-78, 2000.
31 Aneja R, Vangapandu SN, Lopus M, Viswesarappa VG, Dhiman N, Verma A, Chandra R, Panda D and Joshi H: Synthesis of microtubule-interfering halogenated noscapine analogs that perturb mitosis in cancer cells followed by cell death. Biochem Pharmacol *72*: 415-426, 2006.
32 Yarm F, Sagot I and Pellman D: The social life of actin and microtubules: interaction *versus* cooperation. Curr Opin Microbiol *4*: 696-702, 2001.
33 Oshima RG: Intermediate filaments: a historical perspective. Exp Cell Res *313*: 1981-1994, 2007.
34 Takara K, Sakaeda T and Okumura K: An update on overcoming MDR1-mediated multidrug resistance in cancer chemotherapy. Curr Pharm Des *12*: 273-286, 2006.
35 Zhou SF: Structure, function and regulation of P-glycoprotein and its clinical relevance in drug disposition. Xenobiotica *38*: 802-832, 2008.

Received November 13, 2008
Revised January 23, 2009
Accepted February 17, 2009